ELSEVIER

Polymer 44 (2003) 2091–2100

polymer

www.elsevier.com/locate/polymer

The relationship between nano- and micro-structures and mechanical properties in PMMA–epoxy–nanoclay composites

Jong Hyun Park, Sadhan C. Jana*

Department of Polymer Engineering, College of Polymer Science and Polymer Engineering, University of Akron, Akron, OH 44325-0301, USA

Received 20 November 2002; received in revised form 13 January 2003; accepted 15 January 2003

Abstract

Epoxy-aided dispersion of nanoclay particles in a glassy polymer, polymethylmethacrylate (PMMA), was studied using melt-blending technique. Organically treated nanoclay particles were dispersed in PMMA using mixtures of aromatic and aliphatic epoxies to yield three-phase composite materials, the mechanical properties of which were evaluated and compared with PMMA–nanoclay, epoxy–nanoclay, and PMMA–epoxy composite systems as function of nano- and micro-dispersed domains of phase separated epoxy and nanoparticles. Wide-angle-X-ray diffraction patterns and transmission electron microscope images revealed that the clay particles were in fully exfoliated state in the three-phase composites provided the ratio of epoxy to clay was 10. However, the dispersion of nanoclay to the scale of individual platelets was not achieved as exfoliated clay particles remained as aggregates inside phase separated epoxy domains of approximately 1 μm in diameter. Nevertheless, the values of tensile and impact strengths showed significant improvement over PMMA and PMMA–clay composites.

Keywords: Nanocomposites; Epoxy-aided dispersion; Nanoclay

1. Introduction

In the past decade, a spate of research activities on polymer nanocomposites showed great promise for obtaining high performance polymer composite materials with lower density and much increased mechanical strength and stiffness using nanoscale reinforcement. This was amply demonstrated by Toyota researchers for polyamide nanocomposites; well-dispersed single silicate layers augmented the stiffness by as much as 100% and strength by 50% for nanoclay loading of only 4 wt% [1–4]. In addition, a reduction in water absorption by 40% and an increase in heat distortion temperature by 80 °C for the same loading of nanoclay were observed. In separate studies, a 60% increase in storage modulus in glassy region [5] and more than 10-fold increase in strength and modulus in rubbery region [6] have been reported for silicate–epoxy nanocomposites systems. Apart from providing dramatic increase in mechanical properties, the nanoparticles also improve resistance to flammability [7], reduce permeability to small molecules [4,5,8], and cause reduction in solvent uptake [7,9]. A recent review highlighted the methods of synthesis and properties to be achieved from various polymer nanocomposite systems [10].

Some recent studies reported increase of strength and toughness in nanocomposites of glassy polymer matrices, such as polystyrene (PS) and polymethylmethacrylate (PMMA) with layered silicate particles [11–15]. Okamoto et al. [11] observed 200–400% increase in storage modulus for 10 wt% fully exfoliated modified smectic clay dispersed by in situ polymerization of PMMA. Wang et al. [15] reported 20% increase in tensile strength and 50% increase in tensile modulus in in situ emulsion polymerized PMMA with fully exfoliated 3 wt% layered silicate clay. Zeng and Lee [13] exploited the vinyl groups in quaternary ammonium ions for tethering of the particles to polymer chains and achieved fully exfoliated clay structures by in situ free-radical polymerization of methylmethacrylate monomer. While such studies yielded useful knowledge for production of exfoliated clay structures and improvement in mechanical and thermal properties, no indication was given as regards to whether methods based on

* Corresponding author. Tel.: +1-330-972-8293; fax: +1-330-258-2339.
E-mail address: janas@uakron.edu (S.C. Jana).

0032-3861/03/$ - see front matter © 2003 Elsevier Science Ltd. All rights reserved.
doi:10.1016/S0032-3861(03)00075-2

melt-blending of PMMA or other glassy polymers with clay particles would produce similar results.

Melt blending of polymers and inorganic fillers, whether nanoscopic or microscopic, is easy to carry out using conventional compounding means and is more attractive than the methods based on solution blending or in situ polymerization. Nevertheless, melt blending methods are fraught with several issues related to processing difficulties and product quality, for example, severe molecular degradation caused by shear heating or inhomogeneous dispersion of particulate fillers due to poor wetting in high viscosity polymers.

An avenue to utilize the convenience of melt-blending methods without degradation of polymers is to resort to the use of non-solvent type dispersion aids, such as low molecular weight epoxies. Such methodology has been successfully used in the past [9] to disperse nanoscale fumed silica particles in high temperature thermoplastic polymers, such as polyethersulphone (PES) and a reduction in processing temperature by as much as 80 °C was observed due to miscibility of the components. The resultant materials offered significantly reduced solvent uptake due to the presence of fumed silica particles dispersed to the scale of 60 nm.

The miscibility of many thermoplastic polymers with thermosetting epoxies was exploited in a series of studies to establish the 'reactive solvent approach' for processing of intractable polymers [16–21] and to produce dispersed phase morphology varying from a few nanometers to a few micrometers in the same blends by adjustment of the curing conditions [22]. The reactive solvent approach has also been used to produce short and continuous fiber-reinforced composite materials of thermoplastic–thermosetting hybrid matrix polymers [23–26].

In a recent study, Park and Jana [27] investigated the role of elasticity of crosslinked epoxy inside clay galleries and found exfoliated clay structures for $G'/\eta^* \geq 2$ (1/s) and intercalated tactoids for $G'/\eta^* \leq 1$ (1/s), where G' and η^* are, respectively, the values of storage modulus and complex viscosity of the cross-linking epoxy molecules. In view of this and the results reported by Jana and Jain [9] a study was undertaken in our laboratory to investigate the use of epoxies as dispersing agents of nanoclay particles in thermoplastic polymer systems. A representative glassy thermoplastic polymer, PMMA, was chosen as it forms miscible blends with epoxy monomers, thereby causing a reduction of processing temperatures [22]. In addition, organically treated clay particles intercalated with epoxy in the premixed miscible mass with PMMA may potentially yield exfoliated clay structures upon curing of epoxy as has been established separately for nanoclay-reinforced epoxy systems [5,6,8,27–32]. The relevant steps of the methodology used in this study are presented schematically in Fig. 1.

Two important questions about the suitability of the method outlined in Fig. 1 were investigated in this study.

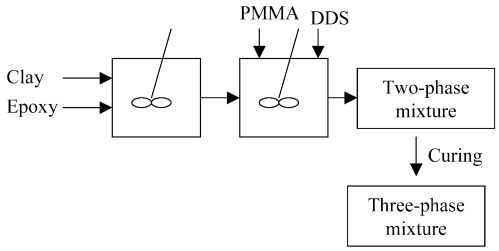

Fig. 1. Schematic of the methodology used in the study.

The first one relates to achieving uniform dispersion of clay particles keeping in mind that separate crosslinked epoxy domains are formed by reaction-induced phase separation of epoxy molecules [9,16–22]. The second question relates to the extent of enhancement in properties to be achieved, for clay particles can potentially produce both intercalated and fully exfoliated states of dispersion in such systems.

2. Experimental methods

2.1. Materials

Cloisite®30B, supplied by Southern Clay Products (Gonzales, TX) with methyl, tallow, bis-2-hydroxyethyl quaternary ammonium ion as the cation exchange resin was used as clay particles. Typically 2% by weight of inherently present moisture was removed before mixing with other ingredients.

Two epoxies, one aromatic and one aliphatic, were mixed in various proportions and used to aid dispersion of nanoclay particles. The aromatic epoxy, diglycidyl ether of bisphenol A (DGEBA), was obtained from Shell Chemical (Houston, TX) in the form of EPON®828 with epoxide equivalent weight of 178–190, viscosity of 11–15 Pa s, and specific gravity of 1.15 at 25 °C. The aliphatic epoxy was polypropylene glycol glycidyl ether in the form of Araldite®DY3601 of Vantico (Brewster, NY) with epoxide equivalent weight of 385–405, viscosity 0.42–0.52 Pa s, and specific gravity 1.03 at 25 °C. Tetra-functional epoxy curing agent, benzenamine, 4,4′-sulfonylbis (DDS), made by Ciba (Tarrytown, NY) with trade name HT976, was chosen to facilitate cross-linking of epoxy molecules. Mixtures of EPON®828 and Araldite®DY3601 were preferred over the use of EPON®828 alone to obtain crosslinked epoxy phase with a glass transition temperature (T_g) much less than that of the PMMA phase so that enhancement in impact toughness can be obtained.

PMMA chosen for the study was obtained from INEOS Acrylics (Cordova, TN) in the form of grade Perspex® CP-80, with $M_z \sim 65\,000$–$85\,000$ and T_g of 110 °C.

2.2. Blend preparation

The epoxy components were mixed in a beaker at room temperature (25 °C) in the weight ratio of 90/10, 80/20, and

70/30, respectively, and cured with stoichiometric quantities of DDS at 200 °C for 3 h.

Cloisite®30B clay particles were mixed with the epoxy mixtures by stirring at 80 °C for 72 h to produce epoxy–intercalated clay mixtures containing 10, 20, and 30 wt% clay. The clay–epoxy mixtures thus produced were dried at 80 °C for 12 h in vacuum oven to remove the traces of moisture. Such large excess of clay were mixed with epoxies primarily to obtain PMMA–epoxy–clay composites with 1–5 wt% clay.

Ground PMMA pellets, dried for 24 h at 80 °C in vacuum oven, were lightly mixed with clay–epoxy mixtures using a spatula to produce a paste, which was dried in vacuum oven for 6 h at 80 °C before mixing in an internal mixer, Brabender Plasticorder at 200 °C for 12 min. A homogeneous material was produced, to which stoichiometric amount (in relation to the epoxy content) of curing agent DDS was added and mixed further for 4 min. PMMA–epoxy blends, without the clay, were prepared in the same manner. PMMA–clay blends, without the epoxy, were prepared by mixing dried clay particles and PMMA pellets at 200 °C for 16 min in Brabender Plasticorder. The PMMA–epoxy ratio in blends with and without clay particles was varied between 90:10, 80:20, and 70:30 by weight.

2.3. Thermal properties and morphology

The glass transition temperatures (T_g) of various materials were evaluated using Dupont DSC, Model 2910 under nitrogen flow. A scan rate of 20 °C/min and temperature in the range of −30–200 °C were used. Thermo-gravimetric analysis was carried out using TGA-2950, made by TA instrument under nitrogen atmosphere.

The state of clay particle dispersion was checked by one-dimensional wide angle X-ray diffraction (WAXD) patterns obtained using Rigaku X-ray diffractometer (Cu; $\lambda = 1.54$ Å) with a tube voltage of 50 kV and tube current of 150 mA. A scanning rate of 5°/min in the range $1.5° \leq 2\theta \leq 25°$ was used. The state of dispersion was also inspected by transmission electron microscopy (TEM) and scanning electron microscopy (SEM). Sample specimens for TEM were microtomed in a Reichert Ultracut Microtome, mounted on 300-mesh copper grids, and TEM pictures taken at 120 kV with TACNAI-12 TEM. The SEM pictures of cold-fractured samples, etched with oxygen plasma and coated with silver, were taken using Hitachi S-2150 SEM at 20 kV.

2.4. Mechanical properties

Specimens for mechanical testing were prepared in compression molds by curing epoxy at 200 °C for 3 h. Tensile tests (ASTM D-638) were performed at room temperature (25 °C) and 50% mean relative humidity using Instron-5567 tensile testing machine (Canton, MA) with a crosshead speed of 5 mm/min. Notched Izod impact properties were evaluated by using Testing Machines Inc. impact tester following ASTM D-256 method. In each case, at least five sample specimens were used to calculate the mean values and standard deviation.

3. Results and discussion

3.1. PMMA/clay composite

Fig. 2 shows tensile properties and Izod impact toughness of melt-blended PMMA–nanoclay composites as function of clay loading. It is observed that tensile modulus increased from 925 MPa for PMMA to 1225 MPa for a composite of PMMA with 3.8 wt% clay. However, the values of both tensile strength and tensile strain at break decreased, respectively, by 50 and 30% for the same loading of clay. The presence of nanoclay particles also caused reduction in impact and tensile toughness values. The value of tensile toughness was calculated from the ratio of the area under force–displacement curve and the area of the fractured surface as used by Janssen et al. [22].

The WAXD patterns presented in Fig. 3 reveal that clay particles were present in an intercalated state in melt-blended PMMA–clay sample specimens. Clay peaks present at $2\theta = 5°$ and $2\theta = 2.5°$ correspond to d-spacing of, respectively, 1.77 and 3.53 nm, even with low, 2 wt% clay as in Fig. 3(b). The TEM image in Fig. 4(a) corroborates this observation by presenting a visual

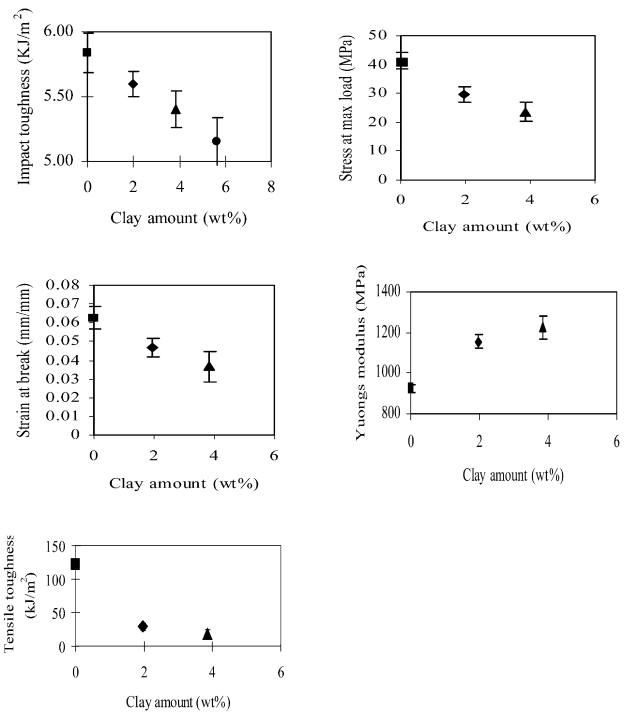

Fig. 2. Effect of clay loading on mechanical properties of melt-blended PMMA–clay composites.

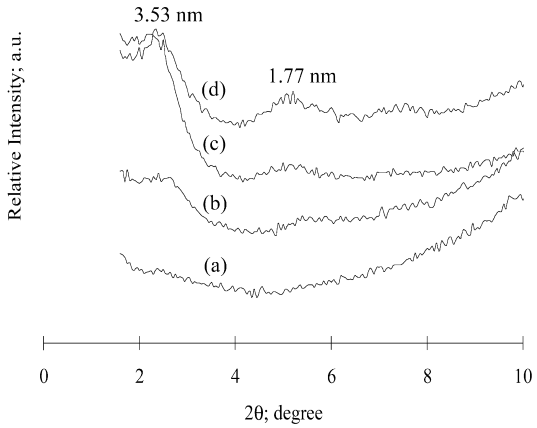

Fig. 3. WAXD patterns of melt-blended PMMA–clay composite with clay content as follows: (a) 0 wt%, (b) 1.96 wt%, (c) 3.85 wt%, and (d) 5.66 wt%.

evidence of the remnant clay tactoid structures. Okamoto et al. [11] and Zeng and Lee [13] reported similar observations for in situ polymerized systems.

The SEM of the fractured surface presented in Fig. 4(b) shows agglomerates of clay particles appearing as white spots, which are distributed evenly in the cross-section. These agglomerates appeared as tactoids in Fig. 4(a). In view of these observations, it can be concluded that melt blending may not be a viable method for dispersion of nanoclay particles in PMMA.

A closer inspection of the fracture surface presented in Fig. 4(b) provides some evidence as regards to the role of the *micro-dispersed* intercalated tactoids on fracture behavior of melt-blended PMMA–clay composites. It is argued that a strong cohesive force among PMMA chains and attractive forces between the adjacent clay particles in tactoids made PMMA–clay interfaces very weak and allowed for crack propagation during facture through the interfaces. This is reflected in lower values of tensile and impact toughness than PMMA with the increase of clay content (Fig. 2).

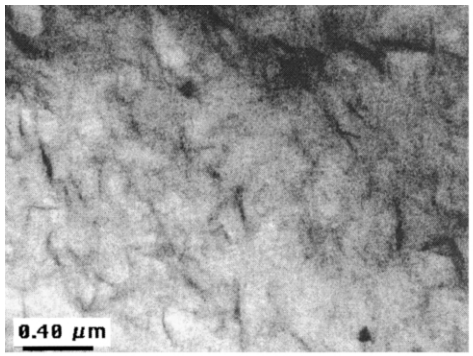

(a)

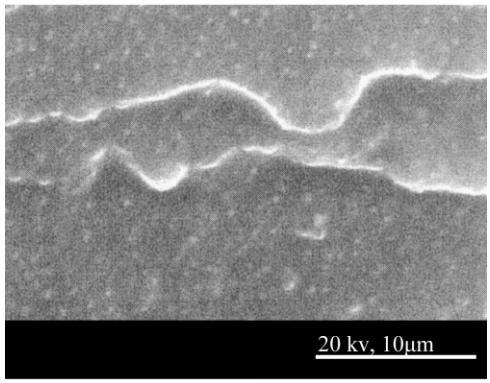

(b)

Fig. 4. State of dispersion of clay structures in melt-blended PMMA–clay composites. (a) TEM image, (b) SEM image for a mixture with 3.85 wt% clay.

3.2. Epoxy–clay composites

Fig. 5 presents the DSC-traces of cured epoxy as function of aliphatic epoxy content. Aliphatic epoxy was mixed with aromatic epoxy to obtain cured epoxy mixtures with a T_g much lower than that of PMMA. A curing time of 3 h at 200 °C guaranteed approximately 97% curing of epoxy in each case. As is evident, the mixture with 30 wt% aliphatic epoxy provided a broad glass transition with a T_g of 69 °C, which is much lower than that of PMMA (110 °C); the onset and end of glass transition, however, occurred at, respectively, 10 and 110 °C. In the rest of the work involving PMMA–epoxy–clay composites, therefore, an epoxy mixture with 30 wt% aliphatic epoxy was used. Another rationale behind using this composition stemmed from the fact that the ratio G'/η^* was found to be greater than 2 (1/s) during curing of epoxy in a rheometer and consequently exfoliated clay structures were produced.

The WAXD patterns of cured epoxy–clay composites containing 7.7 and 15.5 wt% clay are presented in Fig. 6. A largely exfoliated clay structures, except for a small peak at

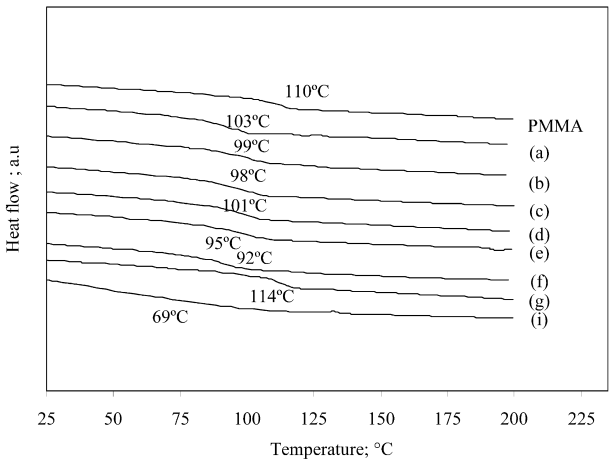

Fig. 5. DSC traces of cured PMMA–epoxy–clay composite. The composition of PMMA, epoxy and clay in parts by weight are as follows: (a) 90:10:1, (b) 80:20:2, (c) 80:20:4, (d) 80:20:6, (e) 70:30:3, (f) 80:20:0, (g) 100:0:2, (i) 0:100:0.

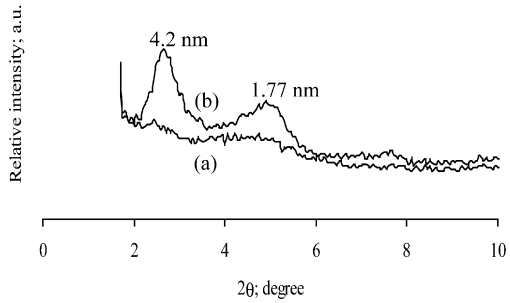

Fig. 6. WAXD patterns of cured epoxy–clay composites with clay content as follows: (a) 7.73 wt%, (b) 15.5 wt%.

$2\theta = 5°$, were obtained in the case of 7.7 wt% clay, while the peaks at $2\theta = 5$ and 2.1° for 15.5 wt% clay indicate the presence of, respectively, organically treated clay and epoxy–intercalated clay structures. The uncured epoxy–clay mixture with 15.5 wt% clay also showed large peaks at $2\theta = 5°$. Therefore, not all clay galleries were intercalated by epoxy in the mixing step for epoxy to clay ratio of 5:1, even though, the minimum weight ratio of epoxy to clay required for complete intercalation is found to be 2:1 by considering epoxy–intercalated gallery height of 3.4 nm.

The exfoliated clay structures produced for systems with epoxy/clay ratio of 10:1 provided large improvements in mechanical properties, as presented in Table 1. For example, more than 150% increase in tensile stress, 20% increase in strain at break, 40% increase in tensile modulus, and, respectively, 240 and 10% increase in tensile and impact toughness were obtained.

3.3. PMMA–epoxy blends

The PMMA–epoxy blends were produced with 90, 80, and 70% by weight of PMMA with T_g values of, respectively, 86, 64, and 45 °C, thereby endorsing complete miscibility before curing of epoxy. Upon curing, the epoxy molecules formed separate domains due to reaction-induced phase separation [9,16,22].

Fig. 7 shows SEM image of the fracture surface of PMMA–cured epoxy blend with 15.5 wt% epoxy, which displays round shaped voids (black spots) occupied by phase separated epoxy domains and mountains (white spots) of the PMMA-phase, indicating a lack of interaction between the PMMA-phase and cured epoxy-phase. The density and size of white and black spots in Fig. 7 corroborate well with the TEM image of the same material presented in Fig. 8. The phase-separated domains of epoxy

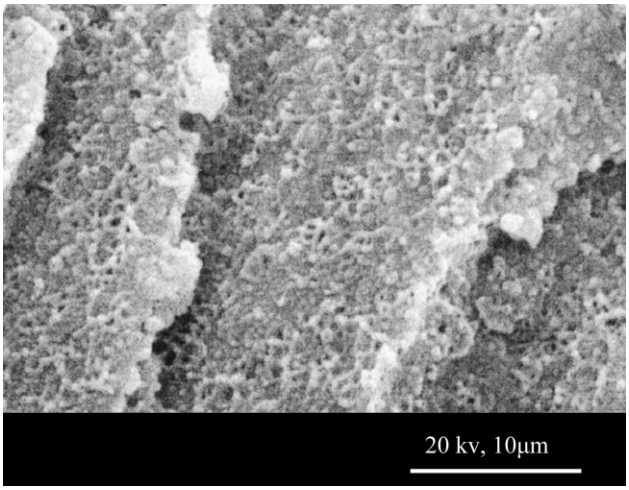

Fig. 7. SEM image of fractured surface of cured PMMA–epoxy blend with 75.6 wt% PMMA and 24.4 wt% epoxy–DDS mixture.

in Fig. 8 are spherical with diameters of 0.1–0.6 μm, while the voids in Fig. 7 range from 0.4–0.6 μm. In addition, the voids of size smaller than 0.4 μm are not apparent in Fig. 7, which endorses a plausible mechanism that cracks must have propagated fast enough through the interface between PMMA phase and larger epoxy domains and not through the interface between PMMA and epoxy domains smaller than 0.4 μm. The smaller epoxy domains, of approximately 0.1 μm in size, absorbed some energy during fast fracture by crack tip blunting effect [33]. This explains slightly higher impact strength values of PMMA–epoxy (6.16 kJ/m^2) systems than PMMA (5.83 kJ/m^2).

In the case of slow crack propagation, such as in tensile tests, the cracks are initiated at the interface between the PMMA and epoxy phases and propagate through the PMMA-phase. If the distance between two adjacent epoxy domains along the crack propagation path is short enough, e.g. under a critical value of 30 nm [22], the composite absorbs more energy than PMMA and prevent premature separation between the phases during tensile test. However, in the current case, the epoxy amount was low (15.5 wt%) and epoxy was cured at 200 °C to achieve high degree of curing. Consequently, the size of epoxy domains was larger and the distance between two adjacent epoxy domains was longer than the critical value of 30 nm. The cracks initiated at the interfaces propagated through the PMMA matrix leading to lower values of tensile stress and strain than PMMA (Table 2). As the glass transition of cured epoxy mixture occurred in a broad range, 10–110 °C, some part of

Table 1
Mechanical properties of epoxy and clay composites

Clay (wt%)	Strain (mm/mm)	Stress (MPa)	Modulus (MPa)	Impact toughness (kJ/m^2)	Tensile toughness (kJ/m^2)
0	0.05	27.2	555	6.5	27
7.7	0.06	69.1	780	7.2	91
15.5	0.04	49.6	1109	7.3	47

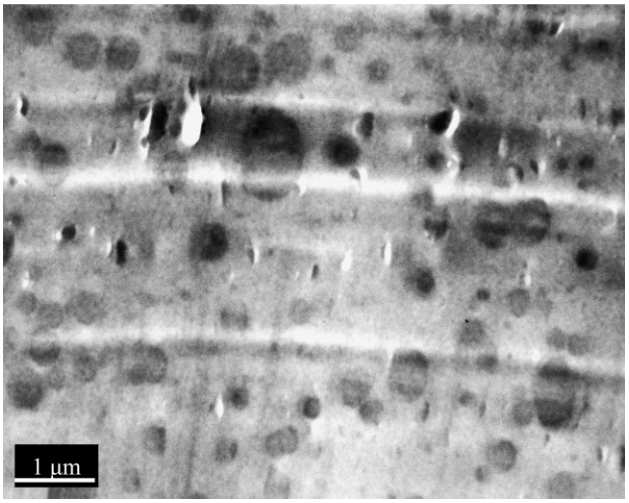

Fig. 8. TEM image of cured PMMA–epoxy blend with 75.6 wt% PMMA and 24.4 wt% epoxy–DDS mixture.

the epoxy phase was in rubbery state at room temperature (25 °C) and absorbed tearing energy during crack propagation, especially in impact tests.

3.4. Blends of PMMA, epoxy, and clay

It is seen above that exfoliated clay particles helped improve the tensile and impact properties of epoxy mixtures, while clay particles in intercalated state in PMMA–clay composites led to deterioration of both tensile and impact strengths. The state of dispersion of clay particles in PMMA–epoxy–clay composites, therefore, would dictate the mechanical properties.

Fig. 9 shows WAXD patterns of PMMA–epoxy–clay composites before curing of epoxy showing peaks corresponding to Cloisite®30B (1.77 nm) and epoxy–intercalated state (4.2 nm) of clay particles. A corresponding TEM image is shown in Fig. 10, which shows clay tactoids with lateral dimensions of 100–200 nm.

The state of dispersion of clay particles after curing of epoxy can be inferred from the inspection of WAXD patterns and TEM images presented in Figs. 11 and 12. The X-ray peaks of curves (a), (b), and (e) in Fig. 11 showed the existence of exfoliated clay morphologies, which is independently evident from the TEM images in Fig. 12. A *d*-spacing of over 8 nm was inferred from the magnified versions of Figs. 12(a) and (b), where clay particles are identified as the darkest phase, while PMMA-matrix and crosslinked epoxy molecules appear, respectively, as light gray and gray. In all these cases, the ratio of epoxy to clay

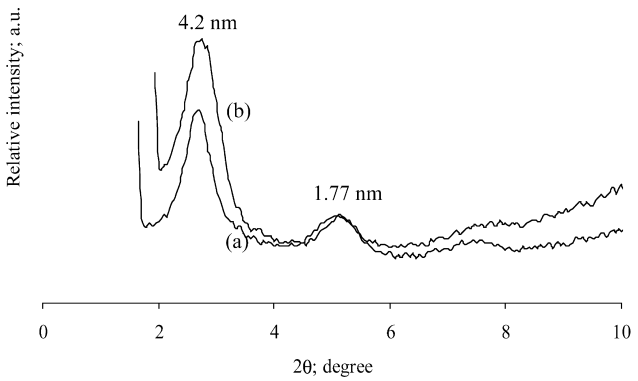

Fig. 9. WAXD patterns of uncured PMMA–epoxy–clay composites. The composition of PMMA, epoxy and clay in parts by weight are as follows: (a) 90:10:1, (b) 80:20:2.

was maintained at 10:1 by weight, in view of the exfoliated clay structures observed in Fig. 6. The X-ray peaks of curves (c) and (d) in Fig. 11 reflect the presence of partially exfoliated clay morphologies with remnant tactoids with *d*-spacing, respectively, of 3.8 and 4.0 nm. In both these cases, the epoxy to clay ratio was less than or equal to 5:1 by weight.

As in Fig. 8, crosslinked epoxy domains were also formed upon curing of epoxy, even in the presence of clay particles. The size of epoxy domains is strongly dependent on the epoxy content as seen in Fig. 12. The largest domains with typical size of 5–10 μm were found in the case of 30 parts of epoxy mixture (Fig. 12(e)), while the smallest domains, ~1 μm, were found with 10 parts of epoxy (Fig. 12(a)).

It is, however, interesting to note that the shape of clay particle agglomerates, whether fully exfoliated or intercalated, dictated the shape of a majority of epoxy domains especially for low epoxy content, such as in Fig. 12(a). In this case, the phase-separated epoxy domains were formed around clay particles already present in the system before curing of epoxy, e.g. those presented in Fig. 10 and, therefore, assumed oblong shapes. Similar epoxy coating layers were reported in the epoxy-aided dispersion of much regular shaped fumed silica particles elsewhere [9]. Not all epoxy domains, however, contain clay particles, such as the spherical domain labeled A in Fig. 12(a).

The shape of phase separated epoxy domains tend to become more spherical with the increase of epoxy content and contain much smaller fraction of clay particles in them, which is especially evident in Fig. 12(e). In view of Figs. 10 and 12, therefore, it can be inferred that the state of dispersion of clay particles, such as the size and distribution

Table 2
Comparison of mechanical properties of PMMA(80 parts)–epoxy(20 parts) blend with PMMA

System	Strain (mm/mm)	Stress (MPa)	Modulus (MPa)	Impact toughness (kJ/m^2)	Tensile toughness (kJ/m^2)
PMMA	0.06	41.3	925	5.8	122
PMMA–epoxy	0.04	26.6	832	6.2	22

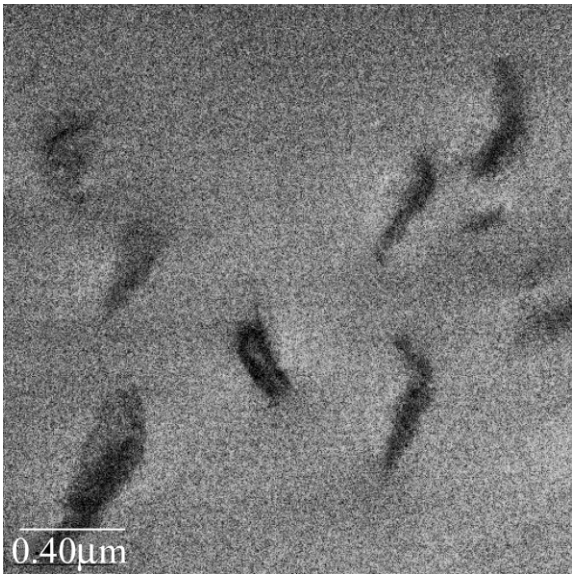

Fig. 10. TEM image of uncured PMMA–epoxy–clay composite with 90 parts PMMA, 10 parts epoxy mixture, 1 part clay.

of tactoids and exfoliated agglomerates in the matrix polymer, does not change upon curing of epoxy. The fully exfoliated clay platelets in Fig. 12(a), (b) and (e) result from curing of epoxy inside the clay galleries of epoxy–intercalated tactoids.

In view of TEM images presented in Figs. 10 and 12, it is clear that the clay particles were not dispersed to the scale of individual platelets, as was the original intention of this work. The TEM image in Fig. 10 especially shows that there were about 25 clay platelets in a typical epoxy–intercalated tactoid, which would produce an exfoliated structure with the same number of platelets upon curing of epoxy, as is the case in Fig. 12(a). This poses an important question as regards to the viability of the epoxy-based dispersion method investigated in this study to produce truly and uniformly nanodispersed system. In the best case scenario presented in this work, fully exfoliated clay structures were

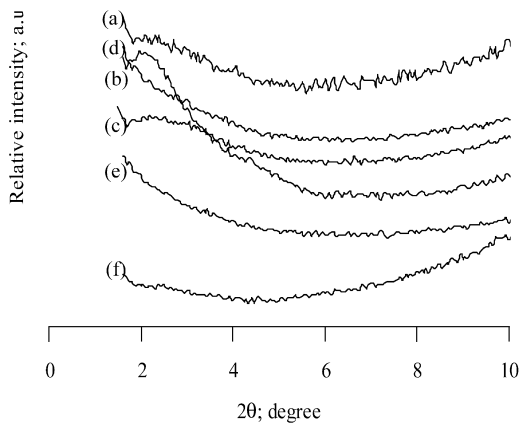

Fig. 11. WAXD patterns of cured PMMA–epoxy–clay composite. The composition of PMMA, epoxy and clay in parts by weight are as follows: (a) 90:10:1, (b) 80:20:2, (c) 80:20:4, (d) 80:20:6, (e) 70:30:3, (f) 100:0:0.

produced when the epoxy to clay ratio was 10 and the separation between the adjacent particles was found to be greater than 8 nm. Nevertheless, the clay particles were not clearly uniformly dispersed throughout the matrix as would be desired. Therefore, it can be argued that dispersion of clay particles to the level of individual clay particles must be carried out even before curing of epoxy, which is a generic problem of melt-blending methods, as shear forces are not always enough to win over the electrostatic and van der Waals forces acting among the particles.

The epoxy component in PMMA–epoxy–clay composites can be cured at the glass transition temperature of the miscible blends to produce nanoscale morphology of phase separated epoxy domains, as demonstrated by Jansen et al. [22]. However, such morphology of the epoxy phase may not be useful in this research in view of the micro-scale dispersed tactoids of uncured blends presented in Fig. 10. The clay particles will remain as agglomerates after curing with the same number of platelets in them as in the uncured system irrespective of whether the epoxy phase forms nanosize or misrosize domains.

Figs. 13 and 14 show the trends of variation of impact and tensile properties as function of clay and epoxy content in cured PMMA–epoxy–clay composites. The maximum reinforcement was found to be with two parts clay in matrix of PMMA and epoxy comprising of 80 parts PMMA and 20 parts epoxy mixture, all by weight. This composition corresponds to Fig. 12(b) with exfoliated clay structures.

As these materials consisted of three phases—PMMA, epoxy, and clay—the resultant mechanical properties should be compared with those of PMMA and PMMA–epoxy to understand the effect of clay particles and phase separated epoxy domains. It is clear that even though the clay particles were contained inside phase-separated epoxy domains and, therefore, not dispersed uniformly inside the PMMA matrix, the measured mechanical properties truly reflect the effect of state of exfoliation or intercalation. For example, the strength and toughness values decreased at 4 parts clay loading, such as for the composition of Fig. 12(c). In this case, the clay particles were found to be in an intercalated state inside the epoxy phase. The values of tensile modulus, however, increased with clay content.

Fig. 14 shows the effect of increase of the epoxy content in the composites on mechanical properties. The ratio of epoxy to clay was maintained at 10. Note that at these compositions, fully exfoliated clay structures were produced and the size of epoxy domains increased with the epoxy content, e.g. in Fig. 12(a), (b), and (e). The values of tensile stress and tensile strain at break increased at higher loading of epoxy although tensile modulus showed dramatic decrease, purportedly due to large excess of softer epoxy phase with lower T_g than PMMA. The values of impact strength showed a maximum at 15.5 wt% epoxy content.

The increase in tensile strength with increase of epoxy content can be attributed to the presence of much softer epoxy phase with clay particles in them, thereby delaying

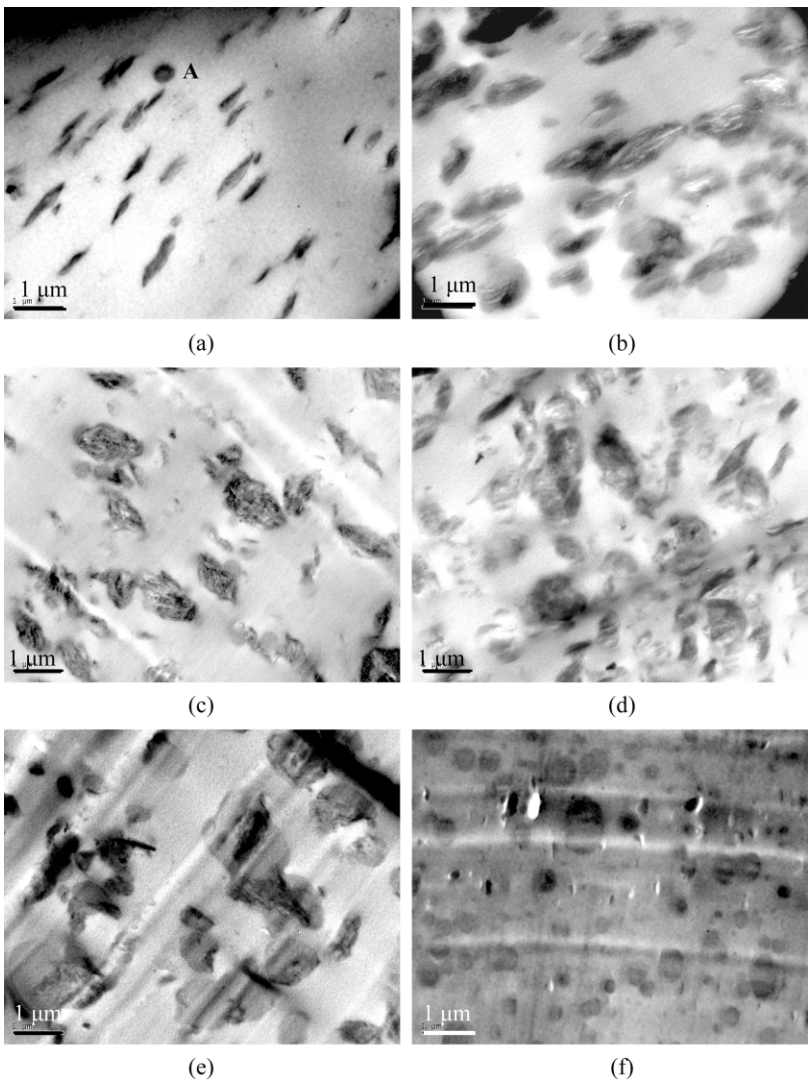

Fig. 12. TEM images of cured PMMA–epoxy–clay composite. The composition of PMMA, epoxy and clay in parts by weight are as follows: (a) 90:10:1, (b) 80:20:2, (c) 80:20:4, (d) 80:20:6, (e) 70:30:3, (f) 80:20:0.

the propagation of crack. However, the Izod impact strength depends on the concentration, i.e. number per unit volume and the size of the dispersed phases as well as on the nature of the dispersed phase itself. For example, in the case of composition of Fig. 12(a), the amount of epoxy phase is not enough to achieve the maximum reinforcement effect, while in the case of composition of Fig. 12(c), the size of the dispersed phase is larger and the cracks propagated along the interface between the PMMA phase and the epoxy phase, instead of involving the clay–epoxy interfaces as well. This is clearly evident from the SEM pictures of the fracture surfaces presented in Fig. 15. The surface morphology of Fig. 15(b) is much more smooth compared to that of Fig. 15(a). It means that the crack propagated along the interface between the epoxy phase and PMMA phase. Since the size of epoxy domains were much smaller in Fig. 15(a), which correspond to the compositions of Fig. 12(b), more surface area was available in Fig. 15(a) for crack propagation.

The presence of clay particles also improved the char content in a thermo-gravimetric analysis as reported in Fig. 16. The epoxy content added to the char content somewhat, but the clay particles contributed much more, especially in the exfoliated state.

4. Conclusions

The use of epoxy as dispersing agent of nanoclay particles in a glassy polymer, PMMA was studied. The clay particles were dispersed to the scale of epoxy–intercalated tactoids with approximately 25 clay platelets in PMMA–epoxy miscible system before curing of epoxy. These tactoids then produced fully exfoliated clay particles upon curing of epoxy when the epoxy to clay ratio was maintained at 10 or remained as tactoids if epoxy to clay ratio was about 5. The clay particles, whether in exfoliated or intercalated states, were found inside the phase-separated

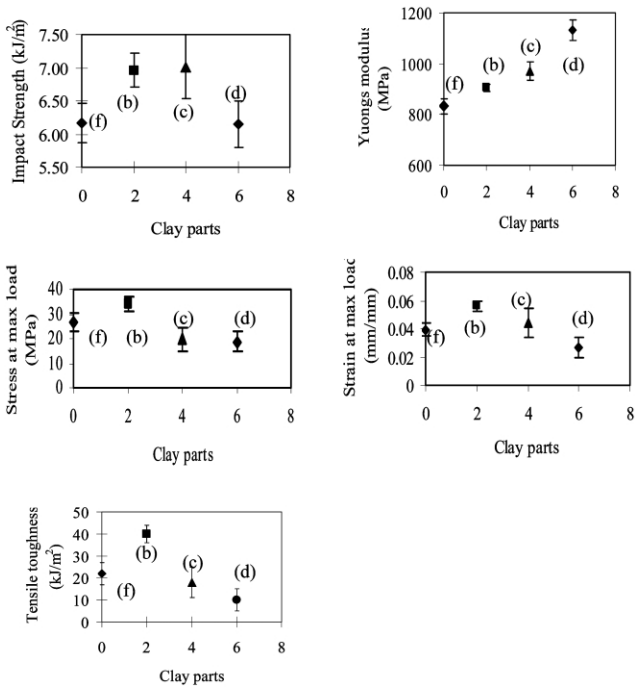

Fig. 13. Effect of clay loading on mechanical properties of cured PMMA–epoxy–clay composites. The letters (b–d) and (f) correspond to the same composition of PMMA, epoxy, and clay in parts by weight as in Fig. 12, i.e. (b) 80:20:2 (c) 80:20:4 (d) 80:20:6 (f) 80:20:0.

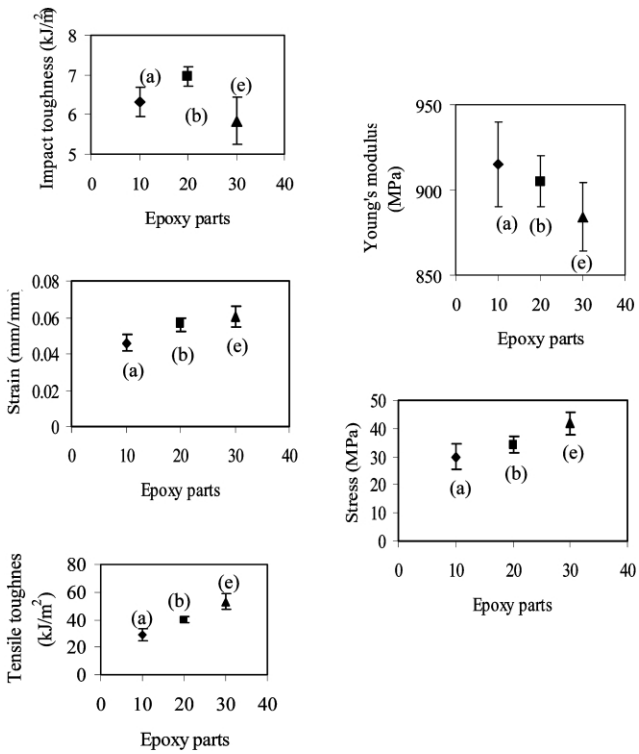

Fig. 14. Effect of epoxy loading on mechanical properties of cured PMMA–epoxy–clay composites. Epoxy to clay ratio was maintained at 10. The letters (a), (b), and (e) correspond to composition of PMMA, epoxy, and clay in parts by weight as in Fig. 12, i.e. (a) 90:10:1, (b) 80:20:2, (e) 70:30:3.

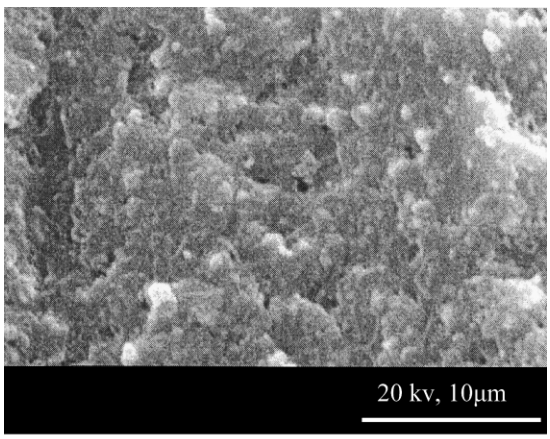

(a)

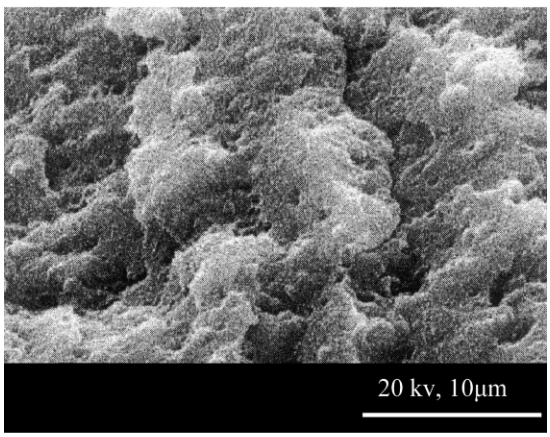

(b)

Fig. 15. SEM images of fractured surfaces of cured PMMA–epoxy–clay composites with the following composition: (a) 80:20:2 (b) 70:30:3, which correspond to the compositions of, respectively, Fig. 12(b) and (e).

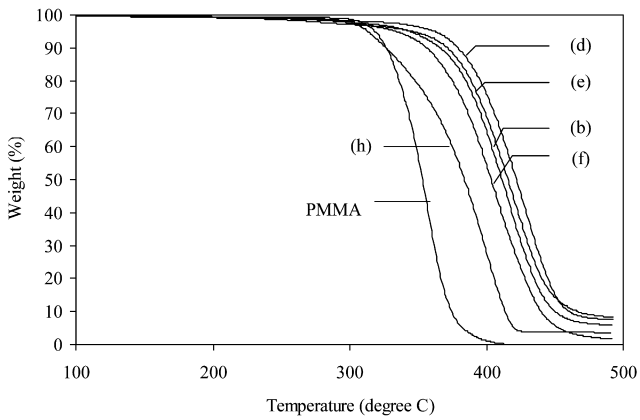

Fig. 16. Results of thermo-gravimetric analysis of cured PMMA–epoxy–clay composites. The letters correspond to composition of PMMA, epoxy, and clay in parts by weight as in Fig. 12, i.e. (b) 80:20:2, (d) 80:20:6, (e) 70:30:3, (f) 80:20:0, (h) 100:0:4.

epoxy domains under all conditions, the size of which grew with the epoxy content.

The microscale structures of clay tactoids in melt-blended PMMA–clay composites deteriorated the mechanical strengths, while the nanoscale exfoliated structure of clay particles in epoxy–clay composites improved their mechanical properties. The phase separated epoxy domains in three-phase PMMA–epoxy–clay systems were microscale and contained clay particles either in exfoliated—therefore, nanodispersed inside the epoxy domains—or in intercalated states. These three-phase composites showed the best properties with two parts of clay content with fully exfoliated clay structures.

It is clear that dispersion of clay particles to the scale of individual platelets would be impossible with the methodology studied. However, the size of the tactoids can be reduced from typically 25 platelets to much smaller numbers through continued mixing under high shear environment. Mixing under high shear environment was not explored in the present study and moreover, viscosity was reduced due to the formation of miscible blends by PMMA and epoxy. One avenue to achieve high shear during mixing in such case is to reduce the mixing temperature, which should help alleviate the concerns of molecular degradation.

It was also noted that the three-phase PMMA–epoxy–clay composites were completely opaque, even though separately produced epoxy–clay composites were completely transparent. Such opacity originated from the mismatch of refractive indices between PMMA and cured epoxy. Nevertheless, effort is underway in our laboratory to produce transparent three-phase systems through proper selection of epoxy, curing agent, and organic treatment, which will be communicated at a later date.

Acknowledgements

The authors acknowledge partial funding of this work from the National Science Foundation in the form of CAREER Award (DMI-0134106). Dr P. Sadhukhan of Bridgstone–Firestone Research is gratefully acknowledged for assistance with the TEM images in Figs. 8 and 10.

References

[1] Usuki A, Kawasumi M, Kojima Y, Okada A, Kurauchi T, Kamigaito O. J Mater Res 1993;8(5):1174–8.
[2] Usuki A, Kojima Y, Kawasumi M, Okada A, Fukushima Y, Kurauchi T, Kamigaito O. J Mater Res 1993;8(5):1179–84.
[3] Kojima Y, Usuki A, Kawasumi M, Okada A, Fukushima Y, Kurauchi T, Kamigaito O. J Mater Res 1993;8(5):1185–9.
[4] Yano K, Usuki A, Okada A, Kurauchi T, Kamigaito O. J Polym Sci: Part A: Polym Chem 1993;31(10):2493–8.
[5] Messersmith PB, Giannelis EP. Chem Mater 1994;6(10):1719–25.
[6] Lan T, Pinnavaia TJ. Chem Mater 1994;6:2216–9.
[7] Burnside SD, Giannelis EP. Chem Mater 1995;7(9):1597–600.
[8] Messersmith PB, Giannelis EP. J Polym Sci A, Polym Chem 1995; 33(7):1047–57.
[9] Jana SC, Jain S. Polymer 2001;42(16):6897–905.
[10] Alexandre M, Dubois P. Mater Sci Engng 2000;R28(1–2):1–63.
[11] Okamoto M, Morita S, Kim YH, Kotaka T, Tateyama H. Polymer 2001;42(3):1201–6.
[12] Lim YT, Park OO. Rheol Acta 2001;40:220–9.
[13] Zeng C, Lee LJ. Macromolecules 2001;34(12):4098–103.
[14] Hwu JM, Jiang GJ, Gao ZM, Xie W, Pan WP. J Appl Polym Sci 2002; 83(8):1702–10.
[15] Wang D, Zhu J, Yao Q, Wilkie CA. Chem Mater 2002;14(9): 3837–43.
[16] Meijer HEH, Venderbosch RW, Goossens JGP, Lemstra PJ. High Perf Polym 1996;8(1):133–67.
[17] Venderbosch RW, Meijer HEH, Lemstra PJ. Polymer 1994;35(20): 4339–57.
[18] Venderbosch RW, Meijer HEH, Lemstra PJ. Polymer 1995;36(6): 1167–78.
[19] Venderbosch RW, Meijer HEH, Lemstra PJ. Polymer 1995;36(15): 2903–13.
[20] Ishi Y, Ryan AJ. Macromolecules 2000;33(1):158–66.
[21] Ishi Y, Ryan AJ. Macromolecules 2000;33(1):167–76.
[22] Jansen BJP, Rastogi S, Meijer HEH, Lemstra PJ. Macromolecules 2001;34(12):3998–4006.
[23] Saalbrink A, Lorteije A, Peijs T. Compos Part A 1998;29A(9–10): 1243–50.
[24] Jana SC, Prieto A. J Appl Polym Sci 2002;86(9):2159–67.
[25] Jana SC, Prieto A. J Appl Polym Sci 2002;86(9):2168–73.
[26] Chandra A. PhD Thesis. University of Akron, in progress.
[27] Park JH, Jana SC. Macromolecules, in press.
[28] Lan T, Kaviratna PD, Pinnavaia TJ. Chem Mater 1995;7:2144–50.
[29] Ishida H, Campbell S, Blackwell J. Chem Mater 2000;12:1260–7.
[30] Wang MS, Pinnavaia TJ. Chem Mater 1994;6:468–74.
[31] Kornmann X, Lindberg H, Berglund LA. Polymer 2001;42:4493–9.
[32] Kornmann X, Lindberg H, Berglund LA. Polymer 2001;42:1303–9.
[33] Lovell PA, McDonand J, Saunders DEJ, Sheratt MN, Young RJ. Adv Chem Ser 1993;233:61–9. Toughened Plastics 1.